


Cite this: *RSC Adv.*, 2021, 11, 35559

Performance and mechanism of conductive magnetite particle-enhanced excess sludge anaerobic digestion for biogas recovery†

Xiaorong Kang  ^a and Yali Liu  ^b

The aim of this study was to evaluate the effect of magnetite particles on the anaerobic digestion of excess sludge. The results showed that methane production increased with the increase in magnetite dosage in the range of 0–5 g L^{−1}, and the cumulative methane production increased by 50.1% at a magnetite dosage of 5 g L^{−1} compared with the blank reactor after 20 days. Simultaneously, numerous volatile fatty acids (VFAs) were produced at high magnetite dosages, providing the required substrates for methanogenesis. The concentration of magnetite addition was positively correlated with methane production, which proved that magnetite was beneficial for the promotion of the conversion of VFAs to methane. Moreover, the degradation efficiencies of proteins and carbohydrates reached 64% and 52.6% at the magnetite dosage of 5 g L^{−1}, respectively, and corresponding activities of protease and coenzyme F420 were 9.03 IU L^{−1} and 1.652 μmol L^{−1}. In addition, the *Methanosaeta* and *Methanoregula* genus were enriched by magnetite, which often participate in direct interspecies electron transfer as electron acceptors.

Received 17th August 2021
Accepted 13th October 2021

DOI: 10.1039/d1ra06236k

rsc.li/rsc-advances

1. Introduction

Excess sludge generated from biological waste water treatment processes has increased continuously in recent decades due to population growth and the construction of new wastewater treatment plants in China.¹ Excess sludge usually contains a large quantity of organic compounds, such as proteins, carbohydrates, cellulose and other organic materials.² Among these, cellulose is the main pollutant of influent suspended solids and accounts for 14–44% of raw excess sludge, where toilet paper is flushed into the sewer system.³

Anaerobic digestion (AD) is the most widely used technology for the successful treatment of excess sludge because it allows for biogas recovery. However, multiple metabolic processes are involved in AD, such as hydrolysis and acidogenesis of complex organic compounds, acetogenesis, and methanogenesis.^{4,5} Among them, the degradation of volatile fatty acids (VFAs) is very important for biogas recovery. As we know, during the AD process, propionic acid degradation is accomplished by syntrophic propionic oxidation ($\text{CH}_3\text{CH}_2\text{COO}^- + 3\text{H}_2\text{O} \rightarrow \text{CH}_3\text{COO}^- + \text{HCO}_3^- + \text{H}^+ + 3\text{H}_{2(\text{g})}$, $\Delta G'^0 = +76.1 \text{ kJ mol}^{-1}$).⁶ Therefore, propionic acid tends to accumulate in the AD system due to its unfavorable thermodynamic properties resulting in

acidification. How to enhance the degradation of volatile acids has become the key to avoid acidification and maintain the stability of the system.

Recently, magnetite particles, as conductive materials, have been applied to the waste treatment process. Ma *et al.*⁷ also found that magnetite could improve the degradation efficiency of an aquatic plant, curly-leaf pondweed. Moreover, the effects of magnetite on the anaerobic co-digestion of pig manure and wheat straw proved that magnetite could enhance methane production and cellulase activity.⁸ The dynamics of VFAs demonstrated that magnetite supplementation enhanced the VFA consumption.⁹ Magnetite has been proven to improve methanogenesis through the direct interspecies electron transfer function.¹⁰ Although magnetite particles were considered to enhance the fermentation process in a variety of environments, the effects of magnetite particles on biogas production and VFA degradation in cellulose sludge fermentation still need to be further studied.

Based on the above-mentioned considerations, the main objective of this study was to assess the effects of magnetite on the AD of excess sludge for biogas recovery. In order to provide a full perspective of the mechanism of magnetite affecting anaerobic performance, special attention was given to the performances of cumulative methane production, the changes in the VFA concentration and component, and the reduction of organic matters. Beside these, key enzyme activities and shifts in the archaea community structure with different magnetite dosages were also investigated.

^aSchool of Environmental Engineering, Nanjing Institute of Technology, Nanjing, 211167, PR China. E-mail: feixiang2004@163.com; Tel: +86-18795465873

^bSchool of Civil Engineering, Nanjing Forestry University, Nanjing, 210037, PR China

† Electronic supplementary information (ESI) available. See DOI: 10.1039/d1ra06236k



2. Material and methods

2.1 Experimental materials

The excess sludge used in this study was obtained from Jiangning Science Park Sewage Treatment Plant (Nanjing, China). After sampling, the excess sludge was mixed and homogenized with a toilet paper obtaining a total concentration of cellulose around 30%, and then, thermal hydrolysis pre-treated at 120 °C for 20 min. The inoculated sludge used in this study was taken from an anaerobic reactor in our laboratory. The characteristics of excess sludge, thermal hydrolysis pre-treated sludge and inoculated sludge are presented in Table 1.

2.2 Batch experiments setup

Batch experiments were performed in five 500 mL reactors with working volume of 450 mL. At the beginning of the experiment, a substrate/inoculum ratio of 0.5 g_{VS}/g_{VS} was inoculated into each reactor. To observe the differences in the methane production caused by magnetite, 0.5, 1, 2 and 5 g L⁻¹ of magnetite particles (Fe₃O₄, diameter of 0.15 mm, purity >98%) were added into the reactors, respectively, and 0 g L⁻¹ of magnetite was used as a blank test. All reactors were capped with rubber stoppers, and flushed with nitrogen gas to remove oxygen before AD. Biochemical methane potential tests were carried out in duplicate at 35 ± 1 °C and 50 rpm for 20 days. The biogas was collected in graduated test tubes, and its volume was measured based on the water displacement.

The pH value in every reactor was measured and adjusted to near neutral pH (7.0–7.5) once a day using 1 M NaOH and 1 M HCl. A 1.5 mL sample of the mixture was taken from each reactor with a syringe every other day, and then centrifuged at 10 000 rpm for 5 min. The supernatant was diluted with deionized water for further measurements.

2.3 Analytical methods

TS, VS and COD were measured according to Standards Methods.¹¹ The pH value was tested by a pH meter (WTW0xi3210, Germany). Carbohydrates were determined using the anthrone sulfuric method with glucose as the standard,¹² and proteins were quantified using a modified Lowry method with bovine serum albumin (BSA) as the standard.¹³ The protease activity was measured using the Forinol method.¹⁴ The coenzyme F420 was analyzed by a UV-visible spectrophotometer at 420 nm.¹⁵ The enzyme involved in sludge was extracted according to the reported method.¹⁶ The VFA

concentrations including acetic, propionic, iso-butyric, butyric, iso-valeric and valeric acids were measured by gas chromatography (Agilent 6890 N).¹⁷ The composition of biogas was determined using gas chromatography (GC-2014, Shimadzu), and the operational parameters and procedures were in accordance with the literature.¹⁸

The inoculum and sludge samples on the 20th day were collected to analyze the archaea community *via* a high-throughput 16S rRNA pyrosequencing, and the detailed DNA extraction, PCR and sequencing methods were mainly based on the literature.¹⁹

2.4 Kinetic analysis of biogas production

The cumulative biogas yield of the anaerobic system was fitted by using the modified Gompertz model (eqn (1)) according to the literature.²⁰

$$P(t) = P_m \exp \left\{ -\exp \left[\frac{R_m e}{P_m} (\lambda - t) + 1 \right] \right\} \quad (1)$$

The detailed parameters are as follows:²¹ $P(t)$ is the cumulative biogas yield (mL g_{VS}⁻¹) at time t ; P_m is the biogas yield potential (mL g_{VS}⁻¹); R_m is the maximum biogas yield rate (mL g_{VS}⁻¹ d⁻¹); λ is the lag phase (d); t is the digestion time (d); and e is a constant (2.71828).

3. Results and discussions

3.1 Methane production

Methane production as the main target production was investigated. Fig. 1a illustrates the changes in the cumulative methane production at different magnetite dosages over time. It is found that the cumulative methane production increased with the increase in time at any magnetite dosage. For example, the cumulative methane production increased from 0 mL to 1408.98 mL at the dosage of 5 g L⁻¹ in 20 days. Moreover, the magnetite dosage also played a positive role in the methane production, and the cumulative methane production enhanced with the increase in the magnetite dosage during the AD process. After 20 days, the cumulative methane productions reached 938.32 mL, 1123.96 mL, 1244.92 mL, 1377.5 mL and 1408.98 mL at magnetite dosages of 0, 0.5, 1, 2 and 5 g L⁻¹, respectively. Compared with the blank reactor, the methane production increased by 19.8–50.1% with the magnetite dosages of 0.5–5 g L⁻¹. As shown in Fig. 1b, the change trends of daily methane production in all reactors were similar, that is,

Table 1 The characteristics of excess sludge, pretreated sludge and inoculated sludge

Item	Unit	Excess sludge	Pretreated sludge	Inoculated sludge
Total solids (TS)	mg L ⁻¹	21 500 ± 250	19 810 ± 210	12.5 ± 0.1
Volatile solids (VS)	mg L ⁻¹	13 100 ± 150	11 040 ± 180	5.7 ± 0.2
Soluble chemical oxygen demand (COD)	mg L ⁻¹	699 ± 50	3621 ± 450	—
Total proteins	mg L ⁻¹	6390 ± 120	—	—
Total carbohydrates	mg L ⁻¹	1580 ± 80	—	—
pH	—	6.5–7.2	—	7.5 ± 0.1



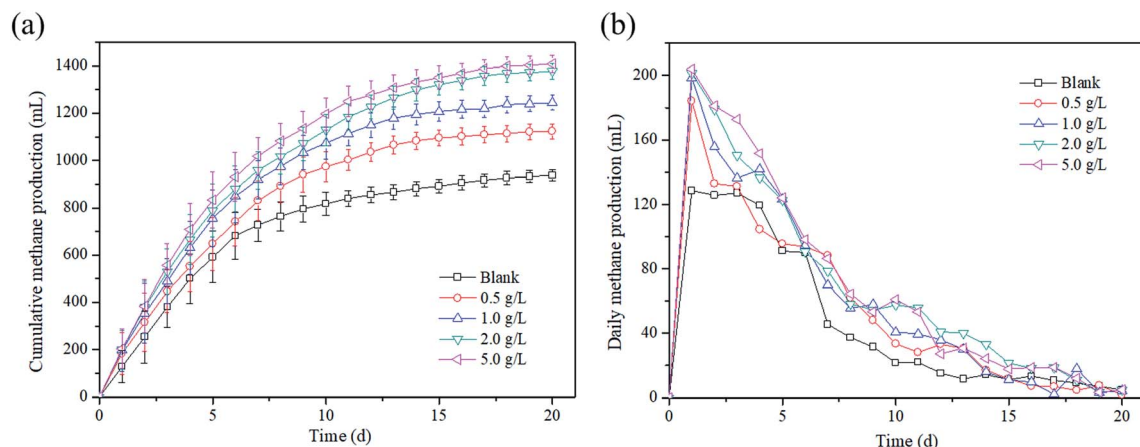


Fig. 1 Effect of magnetite particles dosage on the (a) cumulative methane production and (b) daily methane production.

Table 2 Effects of magnetite particles supplementation on biogas production kinetics

Parameters	Group				
	Blank	0.5 g L ⁻¹	1.0 g L ⁻¹	2.0 g L ⁻¹	5.0 g L ⁻¹
P_m (mL g _{vs} ⁻¹)	69.24	85.36	93.91	104.45	106.03
R_m (mL g _{vs} ⁻¹ d ⁻¹)	9.25	9.55	10.83	10.48	11.74
R^2	0.9927	0.9939	0.9931	0.9891	0.9915

a large amount of methane was produced in the early stage, and then, gradually decreased.

The cumulative biogas yields fitted by a modified Gompertz model are shown in Fig. 1S,[†] and the kinetic parameters are listed in Table 2. The coefficient of determination (R^2) values of the fitted curves was in range of 0.9891 to 0.9939, indicating that the cumulative methane production kinetic was consistent with the modified Gompertz model. The present result was in accordance with previous findings. An increase in the methane production was observed when magnetite was applied for AD of

azo dye waste water.²² The research by Zhao *et al.*²³ also reported that the methane production increased by 29.9% with 10 g L⁻¹ Fe₃O₄ compared with the blank reactor in AD of waste activated sludge. Moreover, similar phenomena were found that the methane production increased to 84 274.7 mL kg_{vs}⁻¹ with 0.5% of Fe₃O₄ nanoparticle dosage.²⁴

The main speculation of promoting methane production by magnetite addition was focused on the dissimilatory iron reduction of magnetite. Due to dissimilatory iron reduction, magnetite can act as an electron acceptor for the hydrolysis of organic matter to accelerate sludge hydrolysis and acidogenesis rate.²⁵ This analysis confirmed the results, and the more organic substrates were provided for methanogens under the higher magnetite dosage (Fig. 2). Moreover, a comparative study of magnetite dosages of 2 g L⁻¹ and 5 g L⁻¹ showed that under the condition that the magnetite dosage increased by 2.5-times, the methane production increased by only 2.3% (Fig. 1a). This phenomenon was consistent with the dominant role of the dissimilatory iron reduction. In the AD process, the Fe(III) reduction obtains more energy than the methanogenesis reaction from the thermodynamic point of view, which leads to the

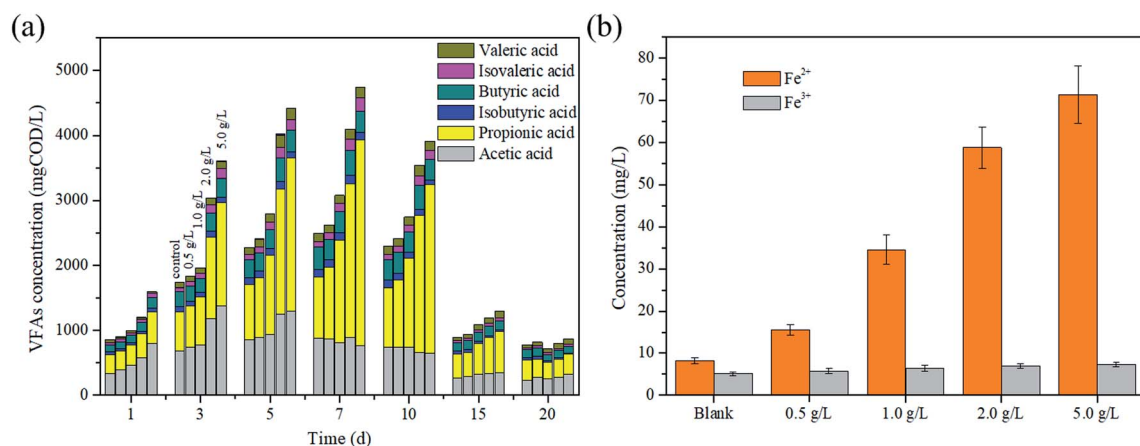


Fig. 2 Effect of magnetite particles dosage on the variation of (a) VFAs and (b) iron ions.

dissimilatory iron reduction is prior to the methanogenesis process.²⁶ The high dosage of magnetite might compete with methanogens for electrons, thereby inhibiting methanogenesis. Thus, it might have an opposite effect on the methanogenesis due to excess iron introduced in the reactor with the addition of magnetite. This speculation is similar to the findings of Suanon *et al.*,²⁴ compared with 0.5% dosage of magnetite, 1% dosage inhibited the methane production in the sludge AD. From the above-mentioned analysis, the reaction of dissimilatory iron reduction played an important role in the process of sludge AD.

Electron transfer was also believed to contribute to methane production, caused by magnetite addition. Magnetite, as an iron oxide with high conductivity, could function as an electron transfer tunnel to achieve interspecies electron transfer between bacteria and methanogens.²⁷ Similar phenomena were found, where metallic oxide played a major role of electron carriers in DIET by transferring the electrons to methanogens in the AD process.²⁸

3.2 Effect of magnetite particles on VFA variation

As the main intermediate products in the acidogenesis step of AD, VFAs are produced from organic matter degradation. The conversion of acetate into methane is responsible for 70% of the methane production in the AD process.²⁹ The variation of the total VFA concentration is presented in Fig. 2a. The result showed that the VFA concentration increased in the initial stage and then decreased. For example, the VFA concentration at a magnetite dosage of 5 g L⁻¹ increased to 4739.7 mg_{COD} L⁻¹ in the first 7 days, and then eventually reduced to 872.91 mg_{COD} L⁻¹. This phenomenon could be explained as follows: numerous organic matters were converted into VFAs at the initial stage owing to thermal pretreatment. Moreover, it was clear to see that the conversion of organic matters to VFAs was enhanced with the increase in the magnetite dosage. The VFA production reached the maximum value on the 7th day in all reactors, and the order of their concentrations were as follows: 5 g L⁻¹ (4739.7 mg_{COD} L⁻¹) > 2 g L⁻¹ (4099.7 mg_{COD} L⁻¹) > 1 g L⁻¹ (3079.8 mg_{COD} L⁻¹) > 0.5 g L⁻¹ (2627.8 mg_{COD} L⁻¹) > the blank reactor (2496.4 mg_{COD} L⁻¹). The reason might be that complex organic matters were decomposed through dissimilatory iron reduction, and the acidification efficiency of excess sludge was improved by magnetite.

As shown in Fig. 2a, acetic and propionic acids were the main components of VFAs. It was observed that on the 7th day, in the reactor of 5 g L⁻¹ magnetite, the acetic and propionic acid concentrations were 1297.77 mg_{COD} L⁻¹ and 2354.72 mg_{COD} L⁻¹, and the corresponding ratios were 29.4% and 53.3%, respectively. The change in the acetic acid concentration confirmed the fact that a large number of substrates were provided for methanogens due to the thermal pretreatment and magnetite addition. It is worth noting that the propionic acid concentration decreased after the 7th day, and the higher magnetite dosage brought out the better degradation efficiency of propionic acid. The result indicated that the magnetite addition influenced the degradation of propionic acid.

The possible reason of how magnetite particles affect the hydrolysis and acidogenesis process was proposed to be *via* the dissimilatory iron reduction. As an iron oxide, magnetite could enrich the Fe(III)-reducing microorganisms that were able to participate in the decomposition of complex organic substrates *via* the dissimilatory iron reduction.³⁰ As a product, Fe²⁺ was detected to reveal the dissimilatory iron reduction. It can be seen from Fig. 2b that the Fe²⁺ concentration increased with an increase in the magnetite dosage. After 20 days, the concentrations of Fe²⁺ were 8.2 mg L⁻¹, 15.5 mg L⁻¹, 34.5 mg L⁻¹, 58.7 mg L⁻¹ and 71.4 mg L⁻¹, respectively. The reduction of magnetite particles to Fe²⁺ showed that numerous electrons produced by the dissimilatory iron reduction might accelerate the hydrolysis of organic compounds. Different from the above, the main reason for propionic acid degradation was that magnetite strengthened the direct interspecies electron transfer because of the good conductive conductivity,³¹ and the Gibbs free energy of DIET (DIET: CH₃CH₂COO⁻ + 0.75H₂O → CH₃COO⁻ + 0.25HCO₃⁻ + 0.25H⁺ + 0.75CH_{4(g)}, ΔG⁰ = -26.4 kJ mol⁻¹ (37 °C, pH 7)) induced by the magnetite addition was more negative than that of the syntrophic propionic oxidation.³²

3.3 Effect of magnetite particles on sludge reduction

As the main components of sludge, proteins and carbohydrates were degraded into simple sugars, amino acids and organic acids in the hydrolysis and acidogenesis process.³³ Thus, the effect of the magnetite dosage on the sludge reduction was characterized by the change in the total protein and carbohydrate concentration. As shown in Fig. 3a, the total protein concentration continued to decrease during the AD process. After 20 days, the protein concentrations were reduced to 3166.9 mg L⁻¹, 2780.2 mg L⁻¹, 2499.4 mg L⁻¹, 2360.3 mg L⁻¹ and 2297.3 mg L⁻¹ at magnetite dosages of 0, 0.5, 1, 2 and 5 g L⁻¹, respectively. The corresponding reduction rates of total proteins were 50.5%, 56.5%, 60.9%, 63.1% and 64%, respectively. Similarly, the change in the total carbohydrates was similar to that of proteins (Fig. 3b), and the concentration of total carbohydrates also decreased continuously. The carbohydrate concentrations were 920 mg L⁻¹, 770.6 mg L⁻¹, 735.5 mg L⁻¹, 693.1 mg L⁻¹ and 679.8 mg L⁻¹ at magnetite dosages of 0, 0.5, 1, 2 and 5 g L⁻¹ after 20 days, respectively. The corresponding reduction rates were 29.9%, 43.5%, 45.4%, 49.1% and 52.6%, respectively.

The decrease in total proteins and carbohydrates with time should be explained as follows: at the beginning, a great number of soluble proteins and carbohydrates were released from sludge due to the thermal hydrolysis pretreatment, which were simultaneously degraded by anaerobic microorganisms for VFA production, leading to the quick reduction of protein and carbohydrate concentration in the first 13 days; in the following AD process, the soluble proteins and carbohydrates were mainly obtained from the biological hydrolysis, and its hydrolysis was equivalent to the acidification rate, resulting in the proteins and carbohydrates remained relatively stable. In addition, the inverse proportional relationship between protein concentration and dosage demonstrated that the sludge



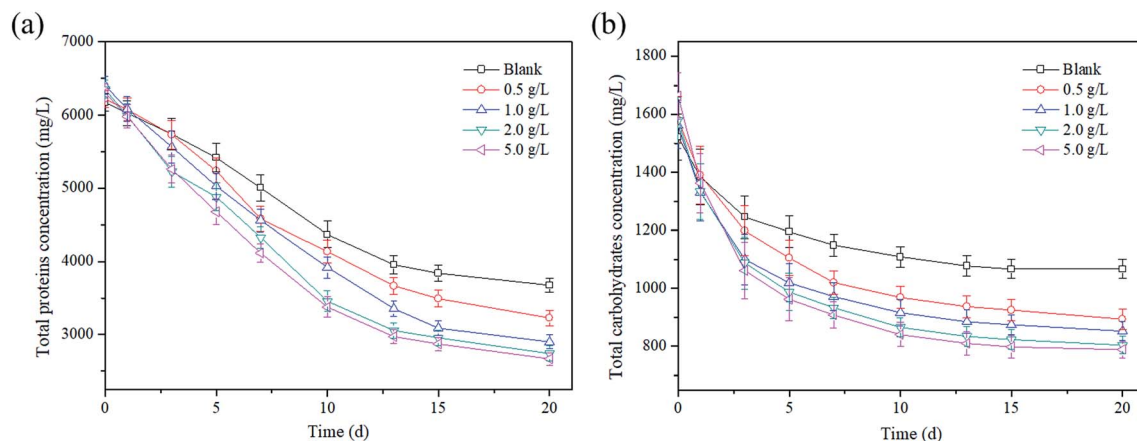


Fig. 3 Effect of magnetite particles dosage on (a) total proteins and (b) total carbohydrates concentrations.

hydrolysis was accelerated effectively by the magnetite addition. Similarly, the research by Zhang *et al.*³⁴ indicated that the reduction rates of proteins and carbohydrates reached 64.9% and 71.4% at a magnetite dosage of 10 g L⁻¹ in the two-phase AD of waste activated sludge.

3.4 Key enzyme activity

To provide a deep insight into the effect of magnetite on the activities of hydrolytic bacteria and methanogens in this study, the concentrations of protease and coenzyme F420 were investigated during the whole AD process. Fig. 4a shows that the change in the protease activity was closely related to the magnetite dosage and the AD time. It was easy to see that the protease activity increased with the extension of time. Taking a dosage of 5 g L⁻¹ as an example, the protease activity increased to 9.03 IU L⁻¹ from 4.8 IU L⁻¹ during the AD process. In addition, it is obvious that the greater the magnetite dosage, the higher the protease activity in AD of excess sludge. It might be that numerous readily degradable proteins were brought into the AD system with thermal pretreatment in initial time, which provided sufficient low molecular weight proteins for hydrolytic bacteria.

As a specific enzyme of methanogens, coenzyme F420 is activated in the electron transfer of methane formation, and has been widely used as an index to reflect the activity of methanogens.³⁵ The coenzyme F420 concentrations increased in initial time and then decreased. Taking the magnetite dosage of 2 g L⁻¹ as an example, the coenzyme F420 concentration increased to 1.637 $\mu\text{mol L}^{-1}$ from 0.982 $\mu\text{mol L}^{-1}$ in the first 5 days, and then decreased to 0.663 $\mu\text{mol L}^{-1}$ on the 20th days. Basically, the coenzyme F420 concentration was enhanced with the increase in the magnetite dosage. In the first 5 days, the F420 concentrations were up to 1.081 $\mu\text{mol L}^{-1}$, 1.201 $\mu\text{mol L}^{-1}$, 1.492 $\mu\text{mol L}^{-1}$, 1.637 $\mu\text{mol L}^{-1}$ and 1.652 $\mu\text{mol L}^{-1}$ at magnetite dosages of 0–5 g L⁻¹, respectively. The activity of coenzyme F420 at a magnetite dosage of 2.0 g L⁻¹ was 1.35-times that of 0.5 g L⁻¹ on the 5th day. It is well known that complicated organic matters cannot be directly utilized by methanogenesis until they are converted to CO₂ or acetate. The addition of magnetite particles into the AD reactor enhanced the hydrolysis and acidogenesis process that produced acetate or CO₂/H₂ for methanogenesis.

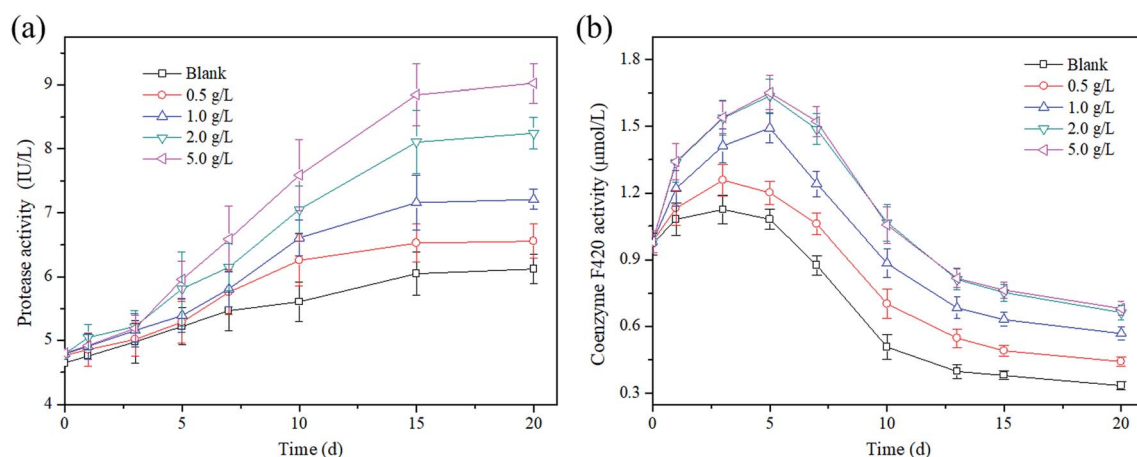


Fig. 4 Effect of magnetite particles on (a) protease activity and (b) coenzyme F420 activity.



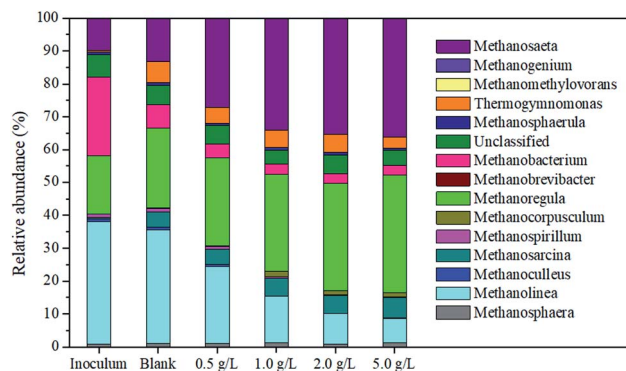


Fig. 5 Effect of magnetite particles on archaea community structure.

3.5 Archaea community structure

The archaea community structure of sludge samples taken from all reactors was investigated. The relative abundance of microbial genus showed that *Methanosaeta*, *Methanoregula* and *Methanolinea* were the dominant genus, whose percentages accounted for 71.84% (blank), 77.2% (0.5 g L⁻¹), 77.7% (1.0 g L⁻¹), 77.39% (2.0 g L⁻¹) and 79.43% (5.0 g L⁻¹), respectively (Fig. 5). Of which, the relative abundance of *Methanosaeta* and *Methanoregula* genus was enhanced with the increase in the magnetite dosage. When the magnetite dosage increased from 0 to 5 g L⁻¹, the percentages of *Methanosaeta* were 13.29%, 27.13%, 34.02%, 35.27% and 36.12%, respectively, and the corresponding percentages of *Methanoregula* were 24.11%, 26.76%, 29.64%, 32.81% and 35.78%. This result indicated that magnetite was beneficial for the enrichment of *Methanosaeta* and *Methanoregula*. *Methanosaeta* was able to dominate the acetoclastic methanogenesis for methane production.³⁶ Abundance of methanogens, acting as an electron acceptor, was enhanced by the metal oxide, and methanogens established biological interspecies electrical connection for the syntrophic metabolism.^{37,38} Even more, *Methanosaeta* participated in the direct interspecies electron transfer as the electron acceptor, and could reduce CO₂ to methane.³⁹ This analysis indicated that the magnetite addition increased the abundance of microbial genus participating in the direct interspecies electron transfer. *Methanolinea* is a hydrogenotrophic methanogen that utilizes H₂ as an electron source for reducing CO₂ into methane.⁴⁰ Therefore, it can be deduced that the abundance of *Methanolinea* decreased gradually in the next reaction mainly using acetic acid as the substrate. *Methanolinea* could perform the direct interspecies electron transfer when it was attached to a conductive support.⁴¹ Some species in the *Methanoregula* genus could utilize formate and hydrogen for methane production in propionate-degrading enrichment culture, which might be related to the degradation of propionic acid.⁴²

4. Conclusions

The valuable effect of magnetite addition on the anaerobic performance of excess sludge with thermal hydrolysis was investigated. The suitable magnetite addition could improve

the methane production significantly by the dissimilatory iron reduction and conductive property. The degradation efficiencies of proteins and carbohydrates were positively correlated with the magnetite dosages. Simultaneously, a large number of VFAs were produced for methanogenesis at a high magnetite dosage, and propionic acid degradation was strengthened by the magnetite addition. In addition, the activities of protease and coenzyme F420 were promoted by a suitable magnetite dosage, explaining the enhanced hydrolysis and the methanogenesis process. It was also found that the magnetite addition was beneficial for the enrichment of *Methanosaeta* and *Methanoregula* involved in the electron transfer.

Author contributions

Xiaorong Kang: conceptualization, data curation, formal analysis, funding acquisition, writing – original draft. Yali Liu: investigation, methodology.

Conflicts of interest

The authors declare that they have no known competing financial interests or personal relationships that could have appeared to influence the work reported in this paper.

Acknowledgements

This research was funded by the Natural Science Foundation of the Jiangsu Higher Education Institutions of China (grant number 16KJB560018), the National Natural Science Foundation of China (grant number 51808282) and the Scientific Research Foundation of the Nanjing Institute of Technology (grant number YKJ201734).

References

- G. Yang, G. Zhang and H. Wang, Current state of sludge production, management, treatment and disposal in China, *Water Res.*, 2015, **78**, 60–73.
- G. Bahreini, E. Elbeshbishy, J. Jimenez, D. Santoro and G. Nakhla, Integrated fermentation and anaerobic digestion of primary sludges for simultaneous resource and energy recovery: impact of volatile fatty acids recovery, *Waste Manag.*, 2020, **118**, 341–349.
- D. Crutchik, N. Frison, A. L. Eusebi and F. Fatone, Biorefinery of cellulosic primary sludge towards targeted short chain fatty acids, phosphorus and methane recovery, *Water Res.*, 2018, **136**, 112–119.
- Y. Abbas, S. Yun, K. Wang, F. Ali Shah, T. Xing and B. Li, Static-magnetic-field coupled with fly-ash accelerant: a powerful strategy to significantly enhance the mesophilic anaerobic-co-digestion, *Bioresour. Technol.*, 2021, **327**, 124793.
- B. Jia, S. Yun, J. Shi, F. Han, Z. Wang, J. Chen, Y. Abbas, H. Xu, K. Wang and T. Xing, Enhanced anaerobic mono- and co-digestion under mesophilic condition: focusing on



- the magnetic field and Ti-sphere core-shell structured additives, *Bioresour. Technol.*, 2020, **310**, 123450.
- 6 G. Capson-Tojo, R. Moscoviz, D. Ruiz, G. Santa-Catalina, E. Trably, M. Rouez, M. Crest, J. P. Steyer, N. Bernet and J. D. Lgenès, Addition of granular activated carbon and trace elements to favor volatile fatty acid consumption during anaerobic digestion of food waste, *Bioresour. Technol.*, 2018, (260), 157–168.
 - 7 D. Ma, J. Wang, T. Chen, C. Shi, S. Peng and Z. Yue, Iron-oxide-promoted anaerobic process of the aquatic plant of curly leaf pondweed, *Energy Fuels*, 2015, **29**(7), 4356–4360.
 - 8 Y. Wang, G. Ren, T. Zhang, S. Zou, C. Mao and X. Wang, Effect of magnetite powder on anaerobic co-digestion of pig manure and wheat straw, *Waste Manage.*, 2017, **66**, 46–52.
 - 9 Q. Yin, K. He, A. Liu and G. Wu, Enhanced system performance by dosing ferroferric oxide during the anaerobic treatment of tryptone-based high-strength wastewater, *Appl. Microbiol. Biotechnol.*, 2017, **101**, 3929–3939.
 - 10 H. Zhuang, J. Shi, S. Shan, L. Ping and C. Zhang, Enhanced anaerobic treatment of azo dye wastewater via direct interspecies electron transfer with Fe₃O₄/sludge carbon, *Int. J. Hydrogen Energy*, 2020, **45**(53), 28476–28487.
 - 11 APHA, *Standard methods for the examination of water and wastewater*, American Public Health Association, 2012.
 - 12 D. L. Morris, Quantitative determination of carbohydrates with dreywood's anthrone reagent, *Science*, 1948, **107**(2775), 254–255.
 - 13 B. Frolund, T. Griebe and P. H. Nielsen, Enzymatic activity in the activated-sludge floc matrix, *Appl. Microbiol. Biotechnol.*, 1995, **43**(4), 755–761.
 - 14 D. Chakraborty, O. P. Karthikeyan, A. Selvam and J. W. C. Wong, Co-digestion of food waste and chemically enhanced primary treated sludge in a continuous stirred tank reactor, *Biomass Bioenerg.*, 2018, **111**, 232–240.
 - 15 G. Bashiri, A. M. Rehan, D. R. Greenwood, J. M. J. Dickson and E. N. Baker, Metabolic engineering of cofactor F-420 production in mycobacterium smegmatis, *PLoS One*, 2010, **5**(12), e15803.
 - 16 Y. Zhao, Y. Chen, D. Zhang and X. Zhu, Waste activated sludge fermentation for hydrogen production enhanced by anaerobic process improvement and acetobacteria inhibition: the role of fermentation pH, *Environ. Sci. Technol.*, 2010, **44**(9), 3317–3323.
 - 17 Y. G. Chen, S. Jiang, H. Y. Yuan, Q. Zhou and G. W. Gu, Hydrolysis and acidification of waste activated sludge at different pHs, *Water Res.*, 2007, **41**(3), 683–689.
 - 18 Y. Cai, X. Zhao, Y. Zhao, H. Wang, X. Yuan, W. Zhu, Z. Cui and X. Wang, Optimization of Fe²⁺ supplement in anaerobic digestion accounting for the Fe-bioavailability, *Bioresour. Technol.*, 2018, **250**, 163–170.
 - 19 Y. Li, Y. Sun, L. Li and Z. Yuan, Acclimation of acid-tolerant methanogenic propionate-utilizing culture and microbial community dissecting, *Bioresour. Technol.*, 2018, **250**, 117–123.
 - 20 K. Wang, S. Yun, T. Xing, B. Li, Y. Abbas and X. Liu, Binary and ternary trace elements to enhance anaerobic digestion of cattle manure: focusing on kinetic models for biogas production and digestate utilization, *Bioresour. Technol.*, 2021, **323**, 124571.
 - 21 B. Li, S. Yun, T. Xing, K. Wang, T. Ke and J. An, A strategy for understanding the enhanced anaerobic co-digestion via dual-heteroatom doped bio-based carbon and its functional groups, *Chem. Eng. J.*, 2021, **425**, 130473.
 - 22 L. Zhuang, J. Tang, Y. Wang, M. Hu and S. Zhou, Conductive iron oxide minerals accelerate syntrophic cooperation in methanogenic benzoate degradation, *J. Hazard. Mater.*, 2015, **293**, 37–45.
 - 23 Z. Zhao, Y. Zhang, Y. Li, X. Quan and Z. Zhao, Comparing the mechanisms of ZVI and Fe₃O₄ for promoting waste-activated sludge digestion, *Water Res.*, 2018, **144**, 126–133.
 - 24 F. Suanon, Q. Sun, D. Mama, J. Li, B. Dimon and C.-P. Yu, Effect of nanoscale zero-valent iron and magnetite (Fe₃O₄) on the fate of metals during anaerobic digestion of sludge, *Water Res.*, 2016, **88**, 897–903.
 - 25 H. Peng, Y. Zhang, D. Tan, Z. Zhao, H. Zhao and X. Quan, Roles of magnetite and granular activated carbon in improvement of anaerobic sludge digestion, *Bioresour. Technol.*, 2018, **249**, 666–672.
 - 26 G. T. Kim, M. S. Hyun, I. S. Chang, H. J. Kim, H. S. Park, B. H. Kim, S. D. Kim, J. W. T. Wimpenny and A. J. Weightman, Dissimilatory Fe(III) reduction by an electrochemically active lactic acid bacterium phylogenetically related to *Enterococcus gallinarum* isolated from submerged soil, *J. Appl. Microbiol.*, 2005, **99**(4), 978–987.
 - 27 C. V. Carolina, R. Simona, F. Stefano, P. Paola, M. Mauro and A. Federico, Magnetite particles triggering a faster and more robust syntrophic pathway of methanogenic propionate degradation, *Environ. Sci. Technol.*, 2014, **48**(13), 7536–7543.
 - 28 J. Chen, S. Yun, J. Shi, Z. Wang, Y. Abbas, K. Wang, F. Han, B. Jia, H. Xu, T. Xing and B. Li, Role of biomass-derived carbon-based composite accelerants in enhanced anaerobic digestion: focusing on biogas yield, fertilizer utilization, and density functional theory calculations, *Bioresour. Technol.*, 2020, **307**, 123204.
 - 29 M. A. Ganzoury and N. K. Allam, Impact of nanotechnology on biogas production: a mini-review, *Renew. Sust. Energ. Rev.*, 2015, **50**, 1392–1404.
 - 30 G. Baek, J. Kim, K. Cho, H. Bae and C. Lee, The biostimulation of anaerobic digestion with (semi) conductive ferric oxides: their potential for enhanced biomethanation, *Appl. Microbiol. Biotechnol.*, 2015, **99**(23), 10355–10366.
 - 31 Y. Wu, S. Wang, D. Liang and N. Li, Conductive Materials in Anaerobic Digestion: From Mechanism to Application, *Bioresour. Technol.*, 2020, **298**, 122403.
 - 32 Y. Jing, J. Wan, I. Angelidaki, S. Zhang and G. Luo, iTRAQ quantitative proteomic analysis reveals the pathways for methanation of propionate facilitated by magnetite, *Water Res.*, 2017, **108**, 212–221.
 - 33 Y. X. Liew, Y. J. Chan, S. Manickam, M. F. Chong, S. Chong, T. J. Tiong, J. W. Lim and G.-T. Pan, Enzymatic pretreatment to enhance anaerobic bioconversion of high strength



- wastewater to biogas: a review, *Sci. Total Environ.*, 2020, **713**, 136373.
- 34 G. Zhang, Y. Shi, Z. Zhao, X. Wang and M. Dou, Enhanced two-phase anaerobic digestion of waste-activated sludge by combining magnetite and zero-valent iron, *Bioresour. Technol.*, 2020, **306**, 123122.
 - 35 D. Wang, Y. Duan, Q. Yang, Y. Liu, B.-J. Ni, Q. Wang, G. Zeng, X. Li and Z. Yuan, Free ammonia enhances dark fermentative hydrogen production from waste activated sludge, *Water Res.*, 2018, **133**, 272–281.
 - 36 A. van Haandel, J. De Vrieze, W. Verstraete and V. S. dos Santos, Methanosaeta dominate acetoclastic methanogenesis during high-rate methane production in anaerobic reactors treating distillery wastewaters, *J. Chem. Technol. Biotechnol.*, 2014, **89**(11), 1751–1759.
 - 37 Z. Wang, S. Yun, J. Shi, F. Han, B. Liu, R. Wang and X. Li, Critical evidence for direct interspecies electron transfer with tungsten-based accelerants: an experimental and theoretical investigation, *Bioresour. Technol.*, 2020, **311**, 123519.
 - 38 S. Yun, T. Xing, F. Han, J. Shi, Z. Wang, Q. Fan and H. Xu, Enhanced direct interspecies electron transfer with transition metal oxide accelerants in anaerobic digestion, *Bioresour. Technol.*, 2021, **320**, 124294.
 - 39 A.-E. Rotaru, P. M. Shrestha, F. Liu, M. Shrestha, D. Shrestha, M. Embree, K. Zengler, C. Wardman, K. P. Nevin and D. R. Lovley, A new model for electron flow during anaerobic digestion: direct interspecies electron transfer to Methanosaeta for the reduction of carbon dioxide to methane, *Energy Environ. Sci.*, 2014, **7**(1), 408–415.
 - 40 S. Sakai, M. Ehara, I. C. Tseng, T. Yamaguchi, S. L. Bruer, H. Cadillo-Quiroz, S. H. Zinder and H. Imachi, *Methanolinea mesophila* sp. nov., a hydrogenotrophic methanogen isolated from rice field soil, and proposal of the archaeal family Methanoregulaceae fam. nov. within the order Methanomicrobiales, *Inter. J. Syst. Evol. Micr.*, 2012, **62**(6), 1389–1395.
 - 41 J.-Y. Lee, S.-H. Lee and H.-D. Park, Enrichment of specific electro-active microorganisms and enhancement of methane production by adding granular activated carbon in anaerobic reactors, *Bioresour. Technol.*, 2016, **205**, 205–212.
 - 42 Y. Yashiro, S. Sakai, M. Ehara, M. Miyazaki, T. Yamaguchi and H. Imachi, *Methanoregula formicica* sp. nov., a methane-producing archaeon isolated from methanogenic sludge, *Inter. J. Syst. Evol. Micr.*, 2011, **61**, 53–59.

